NASA TECHNICAL MEMORANDUM

NASA TM X-52177

NASA TM X-52177

A GENERALIZED CORRELATION OF VAPORIZATION TIMES OF DROPS IN FILM BOILING ON A FLAT PLATE

by Kenneth J. Baumeister, Thomas D Hamill and Glen J. Schoessow
Lewis Research Center
Cleveland, Ohio

TECHNICAL PAPER proposed for presentation at
Third International Heat Transfer Conference
Chicago, Illinois, August 8-12, 1966

NATIONAL AERONAUTICS AND SPACE ADMINISTRATION · WASHINGTON, D.C. · 1966

A GENERALIZED CORRELATION OF VAPORIZATION TIMES OF DROPS IN FILM BOILING ON A FLAT PLATE

by Kenneth J. Baumeister, Thomas D. Hamill
and Glen J. Schoessow

Lewis Research Center
Cleveland, Ohio

TECHNICAL PAPER proposed for presentation at

Third International Heat Transfer Conference
Chicago, Illinois, August 8-12, 1966

NATIONAL AERONAUTICS AND SPACE ADMINISTRATION

A. I. Ch. E.

A GENERALIZED CORRELATION OF VAPORIZATION TIMES OF DROPS IN FILM BOILING ON A FLAT PLATE

by Kenneth J. Baumeister,* Thomas D. Hamill* and Glen J. Schoessow†

Lewis Research Center
National Aeronautics and Space Administration
Cleveland, Ohio

ABSTRACT

A theoretical dimensionless correlation for the vaporization times of discrete liquid masses in the Leidenfrost state is presented and verified experimentally with data in the literature. The correlation is presented as a single curve relating a dimensionless vaporization time to a dimensionless initial liquid volume. The correlation works well for the entire gamut of initial liquid volumes from spherical drops to large pancaked blobs for which experimental data exist.

AUSZUG

Eine theoretische dimensionslose Beziehung für die Verdunstungszeiten diskreter flüssiger Massen im Leidenfrostzustand, die im Versuch mit Angaben im Schrifttum überprüft wurde, wird angegeben. Die Beziehung zeigt sich als eine Einzelkurve des Verhältnisses zwischen einer dimensionslosen Verdunstungszeit und einem dimensionslosem flüssigem Anfangsvolumen. Die Beziehung ist anwendbar auf dem ganzen Bereich flüssiger Anfangsvolumen, von sphärischen Tropfen bis zu flachkugeligen Flecken, für die experimentelle Ergebnisse vorhanden sind.

АННОТАЦИЯ

Приводится и подтверждается экспериментальными данными в литературе, теоретическая безразмерная корреляция времен испарения дискретных жидких масс в состоянии Лейденфроста. Корреляция представляется как единая кривая связывающая безразмерное время испарения с безразмерным начальным объемом жидкости. Корреляция справедлива для всей гаммы начальных объемов жидкости от сферических капель до больших приплюснутых капель для которых имеются экспериментальные данные.

INTRODUCTION

If a quantity of liquid is placed on a sufficiently hot plate, the liquid will evaporate in the immediate vicinity of the plate at a rate sufficient to support the liquid. This phenomenon is referred to in the literature as either Leidenfrost boiling or film boiling. There are two broad categories of general interest that experimental work falls into (Fig. 1):

(1) A continuous or infinite amount of liquid resting on the plate
(2) Discrete or finite amounts (drops) of liquid.

The discrete range (Figs. 1(a) to (e)) has many interesting problems associated with it that are absent from the continuous range. Figure 1 shows a series of possible states that belong to the discrete and the continuous ranges. The additional important variables in the discrete range, which are not associated with the continuous range, are the volume of the liquid mass and the drop shape; that is, the experimentalist working in the discrete range has one additional independent variable, the volume of the liquid placed on the plate. For very small volumes (Fig. 1(a)) the shape of the drop is nearly spherical. With larger volumes (Fig. 1(b)) the drop tends to flatten out into a disk. The thickness of large masses of liquid, called extended drops, tends toward an asymptotic value (Fig. 1(c)). For very large volumes, bubble breakthrough starts occurring (Figs. 1(d) and (e)).

Many of the problems associated with the discrete boiling range are examined in [1 to 11].** In particular, Patel and Bell [7] show that bubble breakthrough (Figs. 1(d) and (e)) is consistent with the prediction of instability theory for submerged surface film boiling. A numerical procedure for calculating the vaporization times of spherical drops (Fig. 1(a)) is presented in [8], while a theoretical analysis of heat transfer to large and extended drops (Figs. 1(b) and (c)) is presented in [5] and [9]. Recently, Baumeister, Hendricks and Hamill showed that metastable Leidenfrost film boiling (Figs. 1(a) to (c)) can occur for plate temperatures as low as the saturation temperature of the liquid [11].

This paper presents a theoretical correlation along with experimental confirmation that allows an a priori prediction of the heat-transfer area, heat-transfer coefficient, and vaporization time for any fluid, wall temperature, and liquid volume.

METHOD OF ANALYSIS

The vaporization time of a discrete liquid drop in Leidenfrost boiling on a flat plate can be found by a direct integration of the interface energy balance:

$$\lambda \rho_L \frac{dV}{dt} = h_T(V) A(V) \Delta T \qquad (1)$$

The functional form of the heat-transfer coefficient will be that presented in [5 and 9]. In

*Lewis Research Center. National Aeronautics and Space Administration, Cleveland, Ohio.

**Numbers in brackets denote references.

†University of Florida, Gainesville, Florida.

these references, a cylindrical model is used to predict the heat transfer. From [9]

$$h_c = 0.68\left(\frac{k^3\lambda^* g\rho_l\rho_v}{\Delta T\mu L_e}\right)^{1/4} \quad (2)$$

where the properties are evaluated at the film temperature,

$$L_e = \frac{V}{\pi^2 l^2} = \text{geometry factor} \quad (3)$$

and

$$\lambda^* = \lambda\left(1 + \frac{7}{20}\frac{c_p\Delta T}{\lambda}\right)^{-3} \quad (4)$$

The heat-transfer expression given by Equation (2) is an analytical expression for the heat-transfer coefficient that would exist if no radiation from the plate to the drop existed; however, radiation is an important heat-transfer mechanism to consider, especially for high plate temperatures. Therefore, the total heat-transfer coefficient to be used in the integration of equation (1) is given by

$$h_T = \frac{h_c}{f} \quad (5)$$

where f is the radiation correction factor. The radiation correction factor f is presented in the Appendix. For convenience and mathematical simplicity, Equation (1) is integrated by using a conductive heat-transfer coefficient rather than the total heat-transfer coefficient. After Equation (1) is integrated, a mean value of the radiative correction factor f is used to give the correct vaporization time.

Equation (1) still cannot be integrated since the heat-transfer area A and effective geometry factor L_e in the heat-transfer expression (Eq. (2)) are unknowns. Thus, the problem of determining these quantities is of paramount importance in computing the vaporization time. A detailed method for computing the shape of the liquid drop by solving the Laplace capillary equation (see Fig. (2)) is presented in [4]:

$$\frac{1}{r_1} + \frac{1}{r_2} = \frac{\Delta P}{\sigma} \quad (6)$$

The Laplace capillary equation relates the surface tension forces and the pressure difference across the surface of a drop. From the drop shape, the geometric parameters A and L_e can be determined.

In summary, the vaporization time for a liquid drop of volume V can be calculated by integration of the interface energy balance given by Equation (1). The procedural steps necessary to perform this integration are as follows:

(1) Solve Equation (6) to determine the shape of the liquid drop for a given liquid volume V in terms of the basic fluid properties.
(2) Determine the heat-transfer area and L_e.
(3) Substitute the value of L_e into the heat-transfer equation (Eq. (2)) thereby giving an expression for the conductive heat-transfer coefficient in terms of the basic fluid properties and the drop volume V.
(4) Substitute the functional form of h_c and A into Equation (1) and integrate for the total vaporization time t_c which assumes only a conductive and convective heat-transfer mode to the drop.
(5) Apply a mean value of the radiation correction factor f (presented in the Appendix) to the expression for the conductive vaporization time to give the actual vaporization time.

DROP SHAPE

A liquid drop not wetting its supporting surface, as in Leidenfrost film boiling, has the general shape depicted in Figure 2. The shape can be found by solution of the Laplace capillary equation (Eq. (6)). Equation (6) was nondimensionalized and transformed into a coupled pair of ordinary nonlinear differential equations, which relate the radius of curvature and the pressure difference at any point on the surface of the drop. The coupled equations were solved by a numerical integration on an IBM 7094 digital computer. The details of the transformation and numerical integration of the equation can be found in [4] along with an experimental verification of the numerical results.

For a given drop volume, the maximum drop radius and an average drop thickness l, defined by the equation

$$l = \frac{V}{\pi r_{max}^2} \quad (7)$$

were determined from the numerical solutions.

The numerical results are shown as a dashed curve in Figure 3. The dimensionless groups shown in Figure 3 are defined as follows:

$$V^* = \frac{V}{\left(\frac{\sigma g_c}{\rho_l g}\right)^{3/2}} \quad (8)$$

$$l^* = \frac{l}{V^{1/3}} \quad (9)$$

From the universal curve, the average drop thickness and maximum radius can be determined provided the surface tension and density of the liquid are known. For purposes of calculation, this curve is broken into three asymptotic ranges.

Extended Drop Domain

The extended drop domain is defined as the domain in which the thickness of the drop is independent of drop volume. For extended liquid drops the universal curve (Fig. 3) approaches a slope of 3, which agrees with the physical observations that the thickness of the drop approaches a constant asymptotic value. From Figure 3 the extended drop region is defined for the domain of V^* where

$$V^* > 155 \quad (10)$$

The average drop thickness in this domain is given by

$$l = 1.85\left(\frac{\sigma g_c}{\rho_l g}\right)^{1/2} \quad (11)$$

This equation is independent of the volume of the drop and provides a method for computing the asymptotic drop thickness.

In addition, according to step 2 in the section METHOD OF ANALYSIS, the heat-transfer area for large cylindrically shaped extended drops can be defined as

$$A = \frac{V}{l} \tag{12}$$

Therefore, when Equation (11) is substituted into Equation (12), the heat-transfer area of an extended liquid drop is

$$A = 0.54V\left(\frac{\sigma g_c}{\rho_l g}\right)^{-1/2} \tag{13}$$

Large Drop Domain

The large drop domain is defined as the domain where the drop is disk-like in shape and where the thickness varies as a function of its volume, as compared with the extended drop whose thickness remains constant. The large drop region exists in the volume range where

$$0.8 < V^* \leq 155 \tag{14}$$

as can be seen in Figure 3. The average drop thickness in this region is

$$l = 0.8\left(\frac{\sigma g_c}{\rho_l g}\right)^{1/4} V^{1/6} \tag{15}$$

In the same manner as in the extended mass region, the heat-transfer area in this region is also defined by Equation (12). Substituting Equation (15) into Equation (12) gives for the heat-transfer area

$$A = 1.25\left(\frac{\sigma g_c}{\rho_l g}\right)^{-1/4} V^{5/6} \tag{16}$$

This equation is applicable for drops intermediate in size, between small spherical drops and extended drops of constant thickness.

Small Drop Domain

When small quantities of liquid are in film boiling on a hot plate, their shape is nearly spherical. Thus, the average drop thickness defined by Equation (7) goes to a limiting value for small spherical drops:

$$l = \frac{V}{A} = \frac{\frac{4}{3}\pi r^3}{\pi r^2} = \frac{4}{3} r \tag{17}$$

But for a sphere

$$V^{1/3} = \left(\frac{4\pi}{3}\right)^{1/3} r \tag{18}$$

Therefore, dividing Equation (17) by Equation (18) gives for small drops

$$l^* = \frac{l}{V^{1/3}} = 0.83 \tag{19}$$

As can be seen in Figure 3, the universal curve approaches this asymptotic value of 0.83. From Figure 3, the small drop domain is taken to exist in that region where

$$V^* \leq 0.8 \tag{20}$$

Thus, in this region the drop thickness is given by

$$l = 0.83\ V^{1/3} \tag{21}$$

The heat-transfer coefficient (Eq. (2)) derived in [9] was based on the assumption that a uniform gap existed beneath the drop; however, this is clearly not the case when a small drop is resting on the surface. Consequently, the effective heat-transfer area is expected to be greater than the projected area of the sphere but less than the surface area of the lower half of the sphere; that is,

$$\pi r^2 < A < 2\pi r^2 \tag{22}$$

Therefore, as an engineering approximation, the effective heat-transfer area of the sphere was taken as the average of the projected and surface areas; that is,

$$A = \frac{\pi r^2 + 2\pi r^2}{2} = 1.5\ \pi r^2 \tag{23}$$

The effect of the preceding approximation was tested against the experimental data of Gottfried [2] and is reported in a later section entitled UNIVERSAL VAPORIZATION TIME PROFILE.

For a sphere,

$$r = \left(\frac{3V}{4\pi}\right)^{1/3} \tag{24}$$

Substituting Equation (24) into Equation (23) gives

$$A = 1.5\left(\frac{3\sqrt{\pi}}{4}\right)^{2/3} V^{2/3} \tag{25}$$

as the effective heat-transfer area of a sphere.

HEAT-TRANSFER COEFFICIENTS

Extended Drop Domain

Substituting the value of l for large drops (Eq. (11)) into Equations (2) and (3) gives

$$h_c = 1.64\left(\frac{k^3\lambda^*\rho_v\sigma g_c}{\Delta T\mu V}\right)^{1/4} \tag{26}$$

for the domain defined by Equation (10). Surprisingly, the heat-transfer coefficient predicted in this case is independent of gravity. Physically, therefore, the gap thickness under an extended liquid drop is independent of the gravitational environment. In a larger gravitational field, however, the drop thickness will be thinner and the heat-transfer area larger, thereby giving rise to shorter vaporization times in large gravitational fields.

Note that the preceding observation does not apply to the near zero-gravity case, since the drop would not obtain an equilibrium position above the plate because of the reactive force of the generated vapor.

Large Drop Domain

Substituting the value of l for large drops and Equation (15) into Equations (2) and (3) gives

$$h_c = 1.075\left(\frac{k^3\lambda^* g^{1/2}\rho_l^{1/2}\rho_v\sigma^{1/2}g_c^{1/2}}{\Delta T\mu V^{2/3}}\right)^{1/4} \qquad (27)$$

for the domain defined by Equation (14).

Small Drop Domain

Substituting the value of l for small drops, Equation (21), into Equations (2) and (3) gives

$$h_c = 1.1\left(\frac{k^3\lambda^* g\rho_l\rho_v}{\Delta T\mu V^{1/3}}\right)^{1/4} \qquad (28)$$

for the domain defined by Equation (20). Note that the heat-transfer coefficient in the small drop domain is independent of surface tension because of the fact that all drops if small enough are spheres independent of the surface tension. The geometry factor L_e appearing in the heat-transfer coefficient is also independent of surface tension for spherical drops.

VAPORIZATION TIMES

Small Drops

The total vaporization time of a liquid drop can be found by a direct integration of Equation (1). Substituting Equations (25) and (28) into Equation (1), integrating, and solving for the vaporization times give

$$t_c = 1.21\left(\frac{\rho_l^3\mu\lambda^4}{k^3 g\lambda^*\rho_v\Delta T^3}\right)^{1/4} V^{5/12} \qquad (29)$$

for the conductive vaporization time.

Thus, according to the definition given to the radiation correction factor of Equation (A1) in the Appendix, the actual total vaporization time is given by

$$t = 1.21\left(\frac{\rho_l^3\mu\lambda^4}{k^3 g\lambda^*\rho_v\Delta T^3}\right)^{1/4} fV^{5/12} \qquad (30)$$

Rewriting the Equation (30) in terms of V^* defined by Equation (8) gives

$$t = 1.21\left(\frac{\rho_l^{1/2}\mu\lambda^4\sigma^{5/2}g_c^{5/2}}{k^3 g^{7/2}\lambda^*\rho_v\Delta T^3}\right)^{1/4} fV^{*5/12} \qquad (31)$$

If a dimensionless total vaporization time t^* is defined as

$$t^* = \frac{t}{f\left(\frac{\rho_l^{1/2}\mu\lambda^4\sigma^{5/2}g_c^{5/2}}{k^3 g^{7/2}\lambda^*\rho_v\Delta T^3}\right)^{1/4}} \qquad (32)$$

the dimensionless total vaporization time for the small drop region is given by the equation

$$t^* = 1.21\ V^{*5/12} \qquad (33)$$

for the domain defined by Equation (20).

Large Drops

Substituting Equations (16) and (27) into Equation (1), evaluating the lower integration limits with Equations (14) and (33), applying the radiative correction factor, and introducing the nondimensional variables defined by Equations (8) and (32) give

$$t^* = 2.23\ V^{*1/3} - 0.97 \qquad (34)$$

for the domain defined by Equation (14).

Extended Drops

Substituting Equations (13) and (26) into Equation (1), evaluating the lower integration limits with Equations (10) and (34), applying the radiation correction factor, and introducing the dimensionless variables defined by Equations (8) and (32) give

$$t^* = 4.52\ V^{*1/4} - 5 \qquad (35)$$

for the domain defined by Equation (10).

Real Time Plots

Figures 4 and 5 present a comparison of the theoretical and experimental total vaporization times for benzene in terms of real time and volume, as calculated from the equations presented in the previous sections.

Theory and experiment are in good agreement for small drops (Fig. 4), for large and extended drops (Fig. 5), and even for drops with bubble breakthrough (10-ml drop).

UNIVERSAL VAPORIZATION TIME PROFILE

A plot of t^* as a function of V^* over the complete range of independent variable V^* is shown in Figure 6. Some of the data in [1,2,4, and 6] have been plotted in terms of the dimensionless variables. The universal relation correlates quite well the available vaporization data over the entire gamut of liquid volumes.

Note that no experimental data found in the literature fall in the small drop range defined by $V^* < 0.8$; however, Gottfried's experimental data came very close to falling in this range.

Even though none of the initial liquid volumes reported in the literature fall into the small drop regime ($V^* < 0.8$) much of Gottfried's data is on the borderline of this limit ($1.5 < V^* < 5.5$). Calculations show that for the smallest V^* reported by Gottfried, the drop spends roughly

75 percent of its life in the small drop domain. The computed vaporization times for Gottfried's data are, therefore, very dependent on the value of the heat-transfer coefficient and area computed for the small drop domain. The verification of the heat-transfer area approximation (Eq. (23)) is based on the agreement of calculated data with Gottfried's data, as shown in Figure 4.

Two empirical correlations derived from dimensional analysis for the vaporization times of small drops are discussed in [2 and 8]. In one correlation Fick's law diffusion coefficient appears; however, the diffusional dependency predicts an infinite evaporation time for experiments conducted in a saturated vapor atmosphere where there is no diffusion [12, p. 376 and 4, p. 8]. This is contrary to fact. The other empirical correlation predicts trends in agreement with the present correlation (Eq. (29)), although the functional dependency of the parameters is different.

DISCUSSION OF RESULTS AND CONCLUDING REMARKS

The generalized correlation (Fig. 6) for prediction of vaporization times of discrete liquid masses presented in this paper is in good agreement with experimental data. Moreover, the validity of the correlation with respect to the volume of the discrete liquid drops placed on the hot surface applies over the whole spectrum of discrete states observed experimentally (Figs. 1(a) to (e)).

Bubble breakthrough as shown in Figures 1(d) and (e) seems to have a relatively minor effect on heat transfer. On the average, a blob of liquid in the extended drop region with bubble breakthrough appears to be equivalent to a flat disk. In all probability, bubble breakthrough does not alter the heat-transfer area. The presence of holes merely increases the perimeter of the bubbly liquid mass while the area remains constant. If the gap thickness beneath the drop remains fairly constant, the heat-transfer coefficient will not be altered very much. The net result appears to be that the total flux of heat input to the bubbly drop is nearly equal to that calculated by assuming no bubble breakthrough. This is not the case for a confined liquid (Fig. 1(f)) since bubble domes decrease the effective heat-transfer area.

The vertical scatter of the data points shown in Figure 6 appears to result from the experimental uncertainties in the measured volume, vaporization time, and surface temperature. Most important, the surface temperature is reported as a constant value even though the actual plate temperature varies because the drop cools the plate [6, p. 33]. Therefore, the experimental spread in the actual data (see Figs. 4 and 5) will be, of course, mirrored in the correlation shown in Figure 6.

The temperature functionality in the universal vaporization time relations adequately correlated the data as seen by the real time plots (Figs. 4 and 5); consequently, inverting the correlation (i.e., computing surface temperatures from observed evaporation times) should give fairly accurate results.

The good agreement with theory tends to substantiate the use of heat-transfer areas obtained by solving the Laplace capillary equation for an isothermal drop.

NOMENCLATURE

A	area, cm^2
C_p	specific heat of vapor at constant pressure, cal/(g)(^oK)
f	radiation correction factor
g	acceleration of gravity, cm/sec^2
g_c	conversion factor, $1(g)(cm)/(dyne)(sec^2)$
h	heat-transfer coefficient, $cal/(sec)(cm^2)(^oK)$
h_c	calculated conductive heat-transfer coefficient, $cal/(sec)(cm^2)(^oK)$
$\bar{h}_c$	average value of h_c during drop lifetime, $cal/(sec)(cm^2)(^oK)$
h_c'	actual conductive heat-transfer coefficient, $cal/(sec)(cm^2)(^oK)$
h_r	radiative heat-transfer coefficient, $cal/(sec)(cm^2)(^oK)$
h_T	total heat-transfer coefficient, $cal/(sec)(cm^2)(^oK)$
k	thermal conductivity of vapor, $cal/(sec)(cm)(^oK)$
L_e	equivalent geometry factor (see Eq. (3)), cm
l	average calculated drop thickness (see Eq. (7)), cm
l^*	dimensionless drop thickness (see Eq. (9))
P	static pressure, $dynes/cm^2$
ΔP	pressure difference across surface, $dynes/cm^2$
r	radius, cm
r_{max}	maximum radius of drop, cm
r_1, r_2	radii of curvature of drop surface, cm
T	temperature, ^oK
ΔT	$T_w - T_s$, ^oK
t	total vaporization time of drop, sec
t^*	dimensionless total vaporization time of drop (see Eq. (32))
t_c	total vaporization time of drop considering conduction (see Eq. (29))
V	drop volume, cu cm
V_o	initial volume of liquid placed on hot plate, cu cm
V^*	dimensionless drop volume (see Eq. (8))
z	distance from plate, cm
δ	gap thickness beneath drop, cm
ϵ_l	liquid emissivity
λ	heat of vaporization, cal/g
λ^*	modified heat of vaporization (see Eq. (4)), cal/g
μ	absolute viscosity of vapor, poise
ρ	density, g/cm^3
σ	surface tension, dynes/cm
$\bar{\sigma}$	Boltzmann constant, 4.876×10^{-8} k cal/(m^2)(hr)($^oK^4$)

Subscripts:

l	liquid
s	evaluated at saturation conditions
v	vapor
w	wall

APPENDIX - EFFECT OF RADIATIVE TRANSPORT ON VAPORIZATION TIMES

The conductive total vaporization time t_c given by Equation (29) has been calculated by assuming that all the heat is transported by conduction and convection in the thin vapor film. Radiative transport has been neglected entirely. When radiation becomes appreciable at about 450° C, the theoretical vaporization times will be high.

For wall temperatures up to about 550° C the following correction factor to t_c is suggested: let t equal the vaporization time when radiation is present. Then, let f be defined by the equation

$$t = ft_c \tag{A1}$$

where f is a factor less than 1 that accounts for radiation.

The factor f is also equal to the mean value of the ratio of the heat-transfer coefficient obtained by neglecting radiation to the coefficient obtained by retaining the radiation term. By extension of the analysis in [9, p. 13, Eq. (45)] the following equation can be shown to be valid in this temperature range:

$$f = \frac{\bar{h}_c}{h_T} = \frac{1}{\left[1 + \frac{1}{4}\frac{h_r}{\bar{h}_c\left(1 + \frac{7}{20}\frac{C_p\,\Delta T}{\lambda}\right)}\right]^3} \tag{A2}$$

where h_r is the radiation heat-transfer coefficient. For the flat disk geometry

$$h_r \approx \frac{\epsilon_l \bar{\sigma}\left(T_w^4 - T_s^4\right)}{T_w - T_s} \tag{A3}$$

The emissivity of the liquid in the temperature range being considered can be taken conveniently as equal to one if data are lacking. The transmissivity of liquid layers greater than a few millimeters in depth is effectively zero, and the reflectivity of liquids for wavelengths in the infrared is quite small [13, p. 371]. Hence, the emissivity is very nearly one.

The plate emissivity does not enter the radiation equation because the ratio of the drop to plate area is effectively zero [2, p. 14]. The bottom surface of the drop "sees" the entire plate; hence, the view factor based on the undersurface of the drop is unity, which leads to Equation (A3).

The heat-transfer coefficient $\bar{h}_c$ should be evaluated at half the initial liquid volume under consideration because heat-transfer coefficient h_c is a weak function of volume, and hence this procedure will give a reasonable estimate of the effect of radiation over the total life of the drop.

Equation (A2) also points out that the heat-transfer coefficients are not simply additive. For small wall temperatures the equation linearizes to

$$h_T = \bar{h}_c + \frac{0.75\,h_r}{\left(1 + \frac{7}{20}\frac{C_p\,\Delta T}{\lambda}\right)} \tag{A4}$$

Note that h_c is not the actual convection coefficient that exists physically. It is a quantity calculated with the assumption that radiation is not present. When radiation is present,

$$-k\left.\frac{\partial T}{\partial z}\right|_{z=\delta} \neq h_c\,\Delta T \tag{A5}$$

because of the nonlinear interaction of radiation and convection-conduction heat transport. Some quantity h_c' exists that does satisfy the equation

$$-k\left.\frac{\partial T}{\partial z}\right|_{z=\delta} = h_c'\,\Delta T \tag{A6}$$

and if this quantity were known, then

$$h_T = h_c' + h_r \tag{A7}$$

However, since h_c is given by a simple formula, a functional relation of the form

$$h_T = f(h_r, h_c) \tag{A8}$$

is more desirable. This is precisely the content of Equation (A4), which should not be misconstrued as a violation of the additivity of coefficients for parallel heat-transfer mechanisms.

REFERENCES

1. Borishansky, V. M.: "Heat Transfer to a Liquid Freely Flowing Over a Surface Heated to a Temperature Above the Boiling Point. Problems of Heat Transfer During a Change of State: A Collection of Articles," Rep. No. AEC-tr-3405, 1953, pp. 109-144.
2. Gottfried, B. S.: "The Evaporation of Small Drops on a Flat Plate in the Film Boiling Regime," Ph.D. Thesis, Case Institute of Technology, 1962.
3. Adadevok, J. K.; O. A. Uyehara; and P. S. Myers: "Droplet Vaporization Under Pressure on a Hot Surface," SAE Paper 701B presented at the S.A.E. Montreal Meeting, June 10-14, 1963.
4. Baumeister, K. J.: "Heat Transfer to Water Droplets on a Flat Plate in the Film Boiling Regime," Ph.D. Thesis, Univ. of Florida, 1964.
5. Baumeister, K. J.; T. D. Hamill; F. L. Schwartz; and G. J. Schoessow: "Film Boiling Heat Transfer to Water Drops on a Flat Plate," A.I.Ch.E. Preprint 24, presented at the ASME-A.I.Ch.E. Eighth National Heat Transfer Conference, Los Angeles, August 8-11, 1965.
6. Patel, B. M.: "The Leidenfrost Phenomenon for Extended Liquid Masses," Ph.D. Thesis, Oklahoma State University, 1965.
7. Patel, B. M.; and K. J. Bell: "The Leidenfrost Phenomenon for Extended Liquid Masses, A.I.Ch.E. Preprint 25, presented at the Eighth National Heat Transfer Conference, Los Angeles, August 8-11, 1965.
8. Gottfried, B. S.; C. J. Lee; and K. J. Bell: "The Leidenfrost Phenomenon: Film Boiling of Liquid Droplets on a Flat Plate," A.I.Ch.E. paper 8a, presented at 57th National Meeting of A.I.Ch.E., Minneapolis, September 26-29, 1965.

9. Baumeister, K. J.; and T. D. Hamill: "Creeping Flow Solution of the Leidenfrost Phenomenon," NASA TN D-3133, December 1965.
10. Poppendiek, H. F.: "Review of the Geoscience Boiling Liquid-Metals Research Program," Paper presented at the 2nd Joint USAEC-Euratom Two-Phase Flow Meeting, Germantown, Maryland, April 1964.
11. Baumeister, K. J.; R. C. Hendricks, and T. D. Hamill, "Metastable Leidenfrost States," NASA TN D-3226, 1966.
12. Kutateladze, S. S.: Fundamentals of Heat Transfer, 2nd Rev. ed., Academic Press, Inc., New York, 1963.
13. Eckert, E. R. G.; and R. M. Drake, Jr: Heat and Mass Transfer, 2nd ed., McGraw-Hill Book Company, New York, 1959.

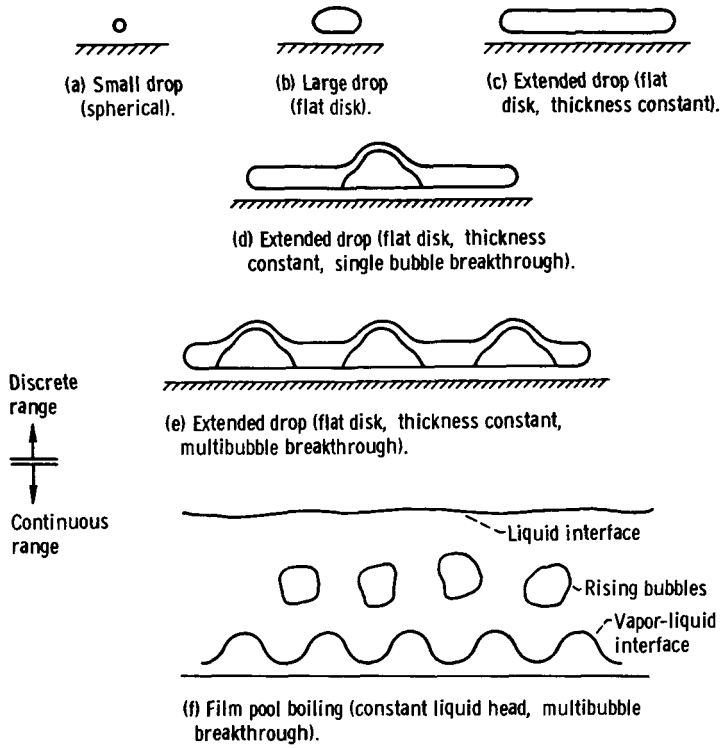

Figure 1. - Film-boiling states of liquid masses.

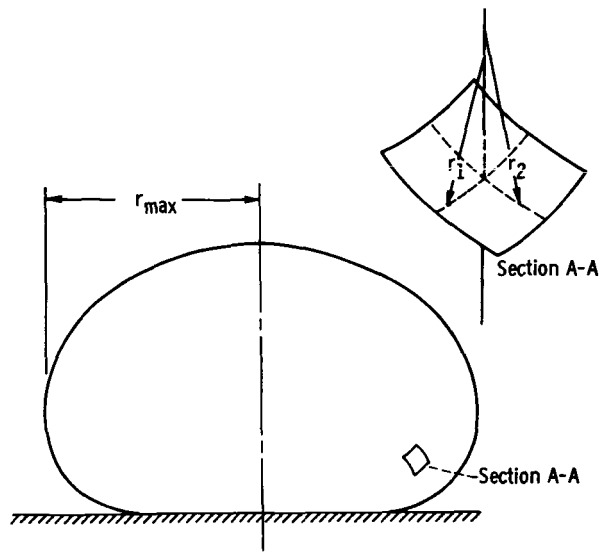

Figure 2. - Schematic of nonwetting liquid drop on flat surface.

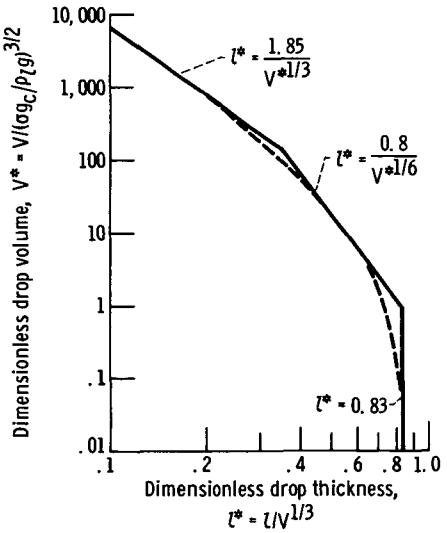

Figure 3. - Universal average drop thickness curve.

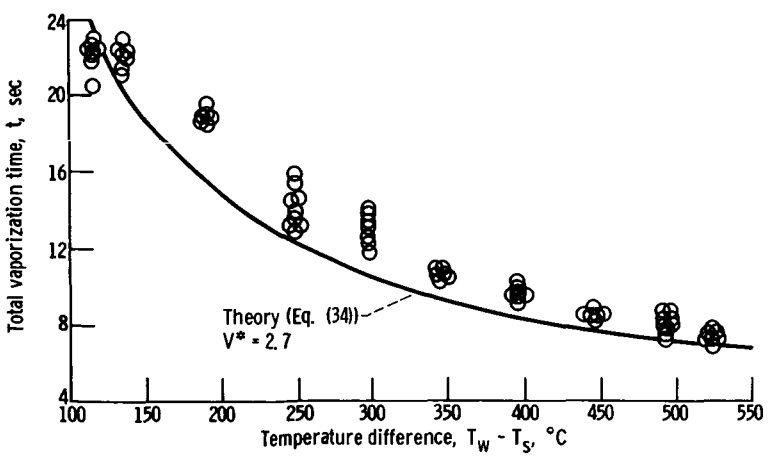

Figure 4. - Droplet vaporization time against temperature difference for benzene. Initial drop volume, $V_0 = 0.0116\ cm^3$ (data from Gottfried [2]).

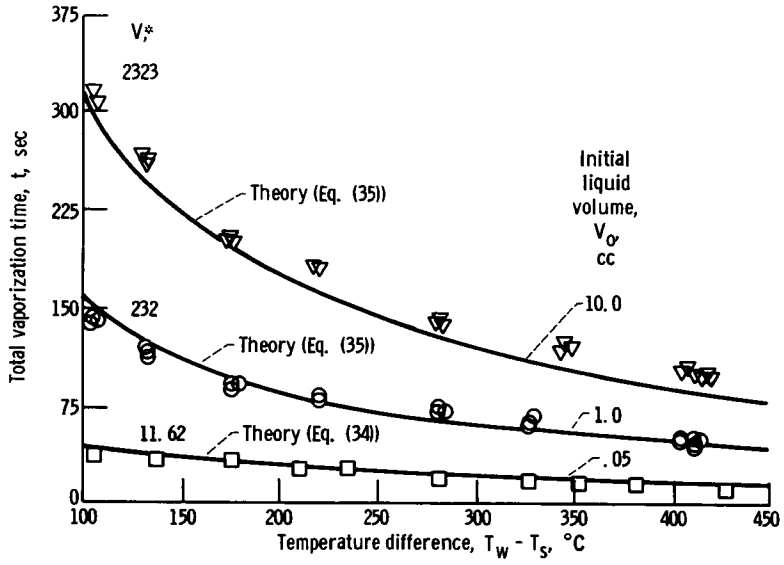

Figure 5. - Liquid vaporization time against temperature difference for benzene (data from Patel and Bell [6 and 7]).

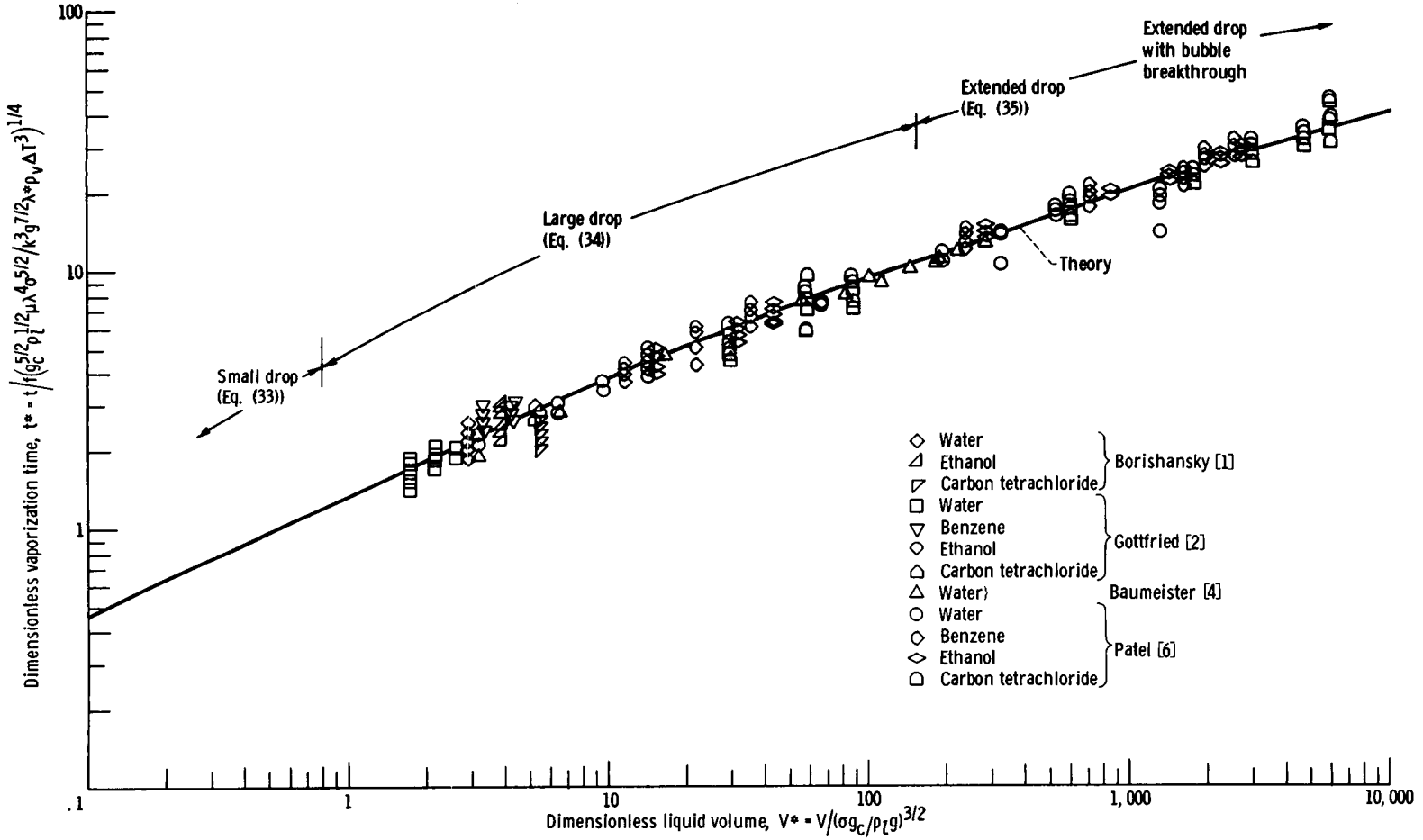

Figure 6. - Universal total vaporization time curve.